AMSE Association for the Advancement of Modelling & Simulation Techniques in Enterprises
IIETA International Information and Engineering Technology Association
Advancing the World of Information and Engineering

Advances in Modelling and Analysis C
Vol. 73, No. 2, June, 2018, pp. 37-44
Journal homepage: http://iieta.org/Journals/AMA/AMA_C

Intelligent condition monitoring of variable speed wind energy conversion systems based on decentralized sliding mode observer

Boumaiza Ahlem*, Arbaoui Fayçal, SaÏdi Mohammed Larbi

Laboratory of Automatic and Signals, Annaba (LASA), Department of Electronics, Badji Mokhtar University, Annaba, P.O. Box 12, Annaba 23000, Algeria

Corresponding Author Email: boumaiza.ahlem@gmail.com

https://doi.org/10.18280/ama_c.730202

Received: 5 April 2018
Accepted: 14 June 2018

Keywords:
convex combination, FDI, polytopic Quasi-LPV modelling, sliding mode observer, state estimation, VSWECS

ABSTRACT

The main objective of this work is to describe the application of Decentralized sliding mode observer (DSMO) based fault detection and isolation (FDI) scheme for nonlinear variable speed wind energy conversion system (VSWECS) designed by a polytopic Quasi LPV representation, which is able to describe it as a convex combination of submodels defined by the vertices of a convex polytope. Stability conditions are performed by using Linear Matrix Inequalities (LMIs). In this work, we focus on the estimation and the reconstruction of the possible actuator and sensor faults to guarantee the efficiency and the continuous operation of this system. Simulation results are given to demonstrate the validity and the effectiveness of the proposed approach.

1. INTRODUCTION

Today, the use of renewable energy has become a strategic, inevitable and necessary choice in front of the unexpected increase of classical energy costs. It is offer natural, economical, clean and safe sources. Wind energy is an example. Its application has made a remarkable progress these last years, providing a considerable production of electrical energy with less spending [1]. During its operation, it involves no rejection and waste [2].

Wind turbines (WT) are attracting increasing attention as alternatives for renewable energy generation; they are the most common wind energy conversion systems (WECS).

The variable speed WECS can be threatened by anomalies which may cause deterioration of its performances or even lead a complete stop of the installation [3]. The condition monitoring status has become essential to ensure its operational safety and availability.

The fault diagnosis procedure is therefore necessary to early predict the apparition of dysfunctions in order to avoid them or to limit their consequences [4]. Several researchers investigated WT fault diagnosis and used, among others, model-based techniques to detect and isolate faults. For example, an FDI is used to control the appearance of fault, and a bank of observer is used to identify the fault kind and its position [5].

Recently, many authors exploited the fuzzy modelling methods for FDI. Park et al [6] have given the design of a robust adaptive fuzzy observer for uncertain nonlinear systems. A new approach to active sensor fault tolerant output feedback tracking control for WT systems via TS model is presented in [7]. Many authors have proposed SMO design methods [8-11].

Walcott and Zak [11] approach necessity a symbolic manipulation package to determine the conception problem which is formulated. To obtain the canonical form, Edwards and Spurgeon [9] give a canonical form for SMO design and a numerically docile algorithm to calculate the gain and the state transformation matrices. Quasi-LPV model predictive reconfigurable control for constrained nonlinear systems is described in [12].

The main challenges of FDI design for WT are: the aerodynamic rotor torque is not measured; and the wind speed is only measured at the hub position with high noise.

In this article, a methodology of diagnosis nonlinear WT system, designated by polytopic Quasi-LPV models using fuzzy observers is proposed. Usually, the conception of a Takagi-Sugeno fuzzy observer need an accurate mathematical description of the process under regard in the form of a polytopic Quasi-LPV dynamic model, which comprises both vertex polytope linear models and activation functions. The vertex polytope linear models are state space affine models that can be derived directly from first principles or from empirical models.

The remainder of this paper is organized as follows: Section 2 describes the nonlinear WT modelling. In section 3 outlines the establishment of a polytopic Quasi-LPV model using the polytopic transformation method to represent the process as a convex combination of submodels determined by the vertices of a convex polytope. These submodels are joined by a convex weighting function to construct the global model. The concept and structure of fuzzy Sliding mode observers and residual generation are presented in Section 4. Several simulation results are presented in Section 5 to show the validity and the effectiveness of this approach. Finally, conclusions and some remarks are drawn and given in Section 6.

2. WIND TURBINE MODELLING

In this part, we present a mathematical model of the WT which is used to design a Quasi-LPV model. We consider a specific variable speed, variable pitch WT model with three blade horizontal axis, and a rating power of 4.8 MW. This

model contains four sub-models: the Blade and Pitch System, the Aerodynamic Model, the Drive Train and the Generator and Converter, as shown in Figure 1 [13].

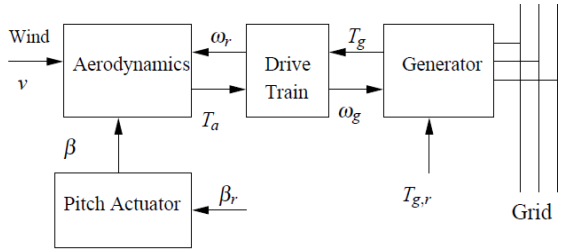

Figure 1. Wind turbine bloc diagram

2.1 Aerodynamic model

The kinetic energy in the wind is captured by turbines and converts it into a torque. The aerodynamic power of the WT P_a and the aerodynamic torque applied to the turbine's rotor T_a are expressed by the following equations:

$$P_a = \frac{1}{2} C_p(\lambda,\beta)\rho\pi R^2 v^3 \tag{1}$$

$$T_a = \frac{1}{2} C_q(\lambda,\beta)\rho\pi R^3 v^2 \tag{2}$$

With:

$$C_q(\lambda,\beta) = \frac{C_p(\lambda,\beta)}{\lambda} \tag{3}$$

where C_q is the thrust coefficient, ρ is the air density, R is the blade length and v is the wind speed λ corresponds to the ratio between the turbine angular speed ω_r and the wind speed

$$\lambda = \frac{\omega_r R}{v}$$

The power coefficient C_p is the turbine aerodynamic efficiency and depends on the tip-speed ratio λ and the blades angle β. It has a lot of values that depend on the type of turbines, and is generally given by the constructor and can be defined by a mathematical approximation [5].

The torque T_a is a nonlinear function of wind speed v, and the power coefficient C_p. C_p is a nonlinear function too, depending on tip speed ratio λ and blades pitch angle β. In the high speed zone, the rotor speed is kept around a nominal speed and then T_a can be approximated as follows:

$$\Delta T_a(t) = \Delta T_{av}(z)\Delta v + \Delta T_{a\beta}(z)\Delta\beta + \Delta T_{a\omega_r}(z)\Delta\omega_r \tag{4}$$

where Δv, $\Delta\beta$, and $\Delta\omega_r$ are the deviations from the operating point where, T_{av} , $T_{a\beta}$ and $T_{a\omega_r}$ are instantaneous partial derivatives of the aerodynamic torque defined as [14]:

$$T_{av}(z) = \left.\frac{\partial T_a}{\partial v}\right|_{(\bar{\omega}_r,\bar{v},\bar{\beta})} = \frac{1}{2}\rho\pi R^2 v\left[2C_p - \lambda\frac{\partial C_p}{\partial\lambda}\right]_{(\bar{\omega}_r,\bar{v},\bar{\beta})}$$

$$T_{a\beta}(z) = \left.\frac{\partial T_a}{\partial\beta}\right|_{(\bar{\omega}_r,\bar{v},\bar{\beta})} = \frac{1}{2}\rho\pi R^2 v^2\left.\frac{\partial C_p}{\partial\beta}\right|_{(\bar{\omega}_r,\bar{v},\bar{\beta})}$$

$$T_{a\omega_r}(z) = \left.\frac{\partial T_a}{\partial\omega_r}\right|_{(\bar{\omega}_r,\bar{v},\bar{\beta})} = \frac{1}{2}\rho\pi R^3 v\left.\frac{\partial C_p}{\partial\lambda}\right|_{(\bar{\omega}_r,\bar{v},\bar{\beta})}$$

$\bar{\omega}_r$, $\bar{v}$ and $\bar{\beta}$ denote the values of rotational speed, wind speed and pitch angle at the operating point, respectively.

2.2 Drive train model

The main role of the drive train is to transfer the aerodynamic torque to the generator to raise the rotational speed according to generator needs.

This model is constructed of a low-speed shaft and a high-speed shaft linked together by the gearbox. The state space model of the drive train is expressed as follows [15]:

$$\begin{bmatrix}\dot{\omega}_r(t)\\ \dot{\omega}_g(t)\\ \dot{\theta}_\Delta(t)\end{bmatrix} = A\begin{bmatrix}\omega_r(t)\\ \omega_g(t)\\ \theta_\Delta(t)\end{bmatrix} + B\begin{bmatrix}T_a(t)\\ T_g(t)\end{bmatrix} \tag{5}$$

$$A = \begin{bmatrix} -\frac{(B_{dt}+B_r)}{J_r} & \frac{B_{dt}}{N_g J_r} & -\frac{K_{dt}}{J_r} \\ \frac{B_{dt}}{N_g J_g} & -\frac{\left(\frac{B_{dt}}{N_g^2}+B_g\right)}{J_g} & \frac{K_{dt}}{N_g J_g} \\ 1 & \frac{-1}{N_g} & 0 \end{bmatrix}$$

$$B = \begin{bmatrix} \frac{1}{J_r} & 0 \\ 0 & -\frac{1}{J_g} \\ 0 & 0 \end{bmatrix}$$

2.3 Pitch system model

The pitch system is composed of three identical pitch actuators. The blade pitch is adjusted by the pitch actuator via rotation. It can be modelled as a second order system:

$$\frac{\beta(s)}{\beta_r(s)} = \frac{\omega_n^2}{s^2 + 2\xi\omega_n s + \omega_n^2} \tag{6}$$

β is the pitch angle $[°]$, β_r is the pitch angle reference $[°]$, ω_n $[rad/s]$ is the natural frequency and ξ $[.]$ is the damping ratio of the pitch actuator model.

Each of the three pitch angle systems has the same transfer function given above. The parameters values of the pitch systems model are identical when no fault appears, these parameters will change in the faulty case.

2.4 Generator and converter model

The mechanical energy is converted by the generator to electric energy, while it is charged by a torque generating from a converter. The converter dynamics can be represented by a first order system [5]:

$$\dot{T}_g(t) = \frac{1}{\tau_g}(T_{g,r} - T_g) \tag{7}$$

$T_{g,r}(t)$ is the reference for the generator torque $[Nm]$, τ_g is the time constant $[s]$.

The power generated by the generator $P_g(t)$ depends on the generator speed $\omega_g(t)$ and the applied load, as described in the equation below:

$$P_g(t) = \omega_g(t) T_g(t) \tag{8}$$

3. DYNAMIC MODEL AND QUASI-LPV REPRESENTATION OF VARIABLE SPEED (WECS)

3.1 The state space model

By using Eq (4) in (5) and including Eq (6) and (7) the augmented nonlinear VSWECS can be formulated as:

$$\begin{cases} \dot{x}(t) = A(z)x(t) + Bu(t) + B_v(z)v(t) \\ y(t) = Cx(t) \end{cases} \tag{9}$$

With

$$x(t) = \begin{bmatrix} \omega_r & \omega_g & \theta_\Delta & \beta & T_g & \dot{\beta} \end{bmatrix}^T$$
$$u(t) = \begin{bmatrix} \beta_r & T_{g,r} \end{bmatrix}^T, y(t) = \begin{bmatrix} \omega_r & \omega_g & \beta & T_g \end{bmatrix}^T, z(t) = \begin{bmatrix} v, \beta \end{bmatrix}^T$$

where: $x(t)$ is the state vector, $u(t)$ is the control input vector, $y(t)$ is the output vector and z represents the nonlinearities. The control system deed both on generator in order to apply the reference electromagnetic torque $T_{g,r}$ and on the pitch actuator system to control the blades pitch angle β.

$$A(z) = \begin{bmatrix} b_1 & \frac{B_{dt}}{N_g J_r} & -\frac{K_{dt}}{J_r} & a_1 & 0 & 0 \\ \frac{B_{dt}}{N_g J_g} & \frac{-b_2}{J_g} & \frac{K_{dt}}{N_g J_g} & 0 & \frac{-1}{J_g} & 0 \\ 1 & \frac{-1}{N_g} & 0 & 0 & 0 & 0 \\ 0 & 0 & 0 & 0 & 0 & 1 \\ 0 & 0 & 0 & 0 & \frac{-1}{\tau_g} & 0 \\ 0 & 0 & 0 & -\omega_n^2 & 0 & -2\xi\omega_n \end{bmatrix}$$

$$B = \begin{bmatrix} 0 & 0 \\ 0 & 0 \\ 0 & 0 \\ 0 & 0 \\ 0 & \frac{1}{\tau_g} \\ \omega_n^2 & 0 \end{bmatrix}, \quad B_v(z) = \begin{bmatrix} a_2 \\ 0 \\ 0 \\ 0 \\ 0 \\ 0 \end{bmatrix} \tag{10}$$

With:

$$a_1 = \frac{1}{J_r}\frac{\partial T_a}{\partial \beta}, \quad a_2 = \frac{1}{J_r}\frac{\partial T_a}{\partial v},$$
$$b_1 = -\frac{(B_{dt} + B_r)}{J_r}, \quad b_2 = \frac{B_{dt}}{N_g^2} + B_g$$

From the state space model it is clear that the system matrix $A(z)$ and the disturbance matrix $B_v(z)$ are not fixed matrices and depend on the state variables. In order to get the best possible representation from this highly nonlinear system, the next subsection presents a Quasi-LPV representation of the system in Eq (9).

3.2 Polytopic quasi-LPV model representation

This approach consists to apprehend the overall behaviour of the system by an ensemble of local models. Each of them characterizes the system's behaviour in a particular operating zone. The local models are then regrouped by means of an interpolation mechanism. The LPV models describe how the system dynamics vary as a function of one or more scheduling varying parameters. When the variation of the scheduling parameters depends on the state space variables and/or input variables, they are denoted Quasi-LPV. The use of this approach permits transferring and generalizing several methods developed in the linear monitoring field to the nonlinear systems and gives good approximation properties which can be used for monitoring.

In this study the dynamic Quasi-LPV model is used to represent the nonlinear system of the Eq.(9) by using the polytopic transformation to describe the system as a convex combination of sub models defined by the vertices of a convex polytope described by the following equation:

$$\begin{cases} \dot{x}(t) = A(z)x(t) + B(z)u(t) \\ y(t) = C(z)x(t) \end{cases} \tag{11}$$

where: $A \in \Re^{n \times n}$, $B \in \Re^{n \times m}$ and $C \in \Re^{p \times n}$ are the state space matrices with variable parameters and z represents the scheduling vector around the equilibrium point.

Function of the *ith* LTI model (see Table 1); $z(t)$ is the scheduling variable: A_i, B, B_{vi} and C are system matrices with suitable dimensions.

The Quasi-LPV model is derived depending on two scheduling variables: the pitch angle $z_1(t) = \beta$ and the wind speed $z_2(t) = v$. These scheduling variables in WT are supposed varying in the operating range: $d_1 \le z_1(t) \le D_1$ and $d_2 \le z_2(t) \le D_2$.

For z_1 and z_2 there exist four functions:

$$O_1 = \frac{z_1 - d_1}{D_1 - d_1}, \quad \bar{O}_1 = \frac{D_1 - z_1}{D_1 - d_1}, \quad O_2 = \frac{z_2 - d_2}{D_2 - d_2}, \quad \bar{O}_2 = \frac{D_2 - z_2}{D_2 - d_2} \tag{12}$$

where:

$O_1 + \bar{O}_2 = 1$ and $O_2 + \bar{O}_2 = 1$ such as:
$z_1(t) = O_1 D_1 + \bar{O}_1 d_1$ and $z_2(t) = O_2 D_2 + \bar{O}_2 d_2$

For simplification, let us denote O_j in the general form:

$$O_j = \frac{-d_j}{D_j - d_j} + \left(\frac{1}{D_j - d_j} \right) z_j(t), \quad \overline{O}_j = 1 - O_j \tag{13}$$

With:

$$D_j \equiv \max_{z_j \in [l_{j\min}, l_{j\max}]} z_j(t), \quad d_j \equiv \min_{z_j \in [l_{j\min}, l_{j\max}]} z_j(t)$$

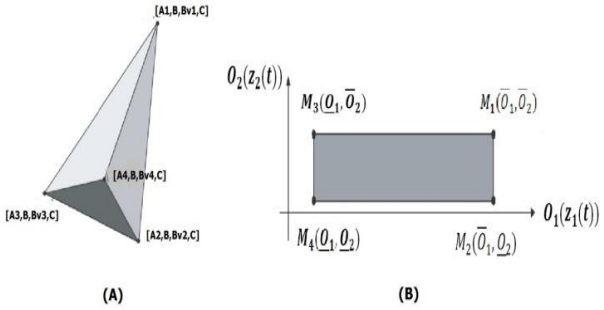

Figure 2. (A) Polytopic space with four vertices, (B) Convex operating zone of the system

For $j = 1,\ 2$ note that $l_{j\min}$ and $l_{j\max}$ are the lower and upper bounds of the variable z_j, respectively.

Then, to obtain the polytopic Quasi-LPV model the scheduling functions of $z_1(t)$ and $z_2(t)$ should be chosen such that:

$$A(z) = \sum_{i=1}^{M} h_i(z(t)) A_i, \quad B_v(z) = \sum_{i=1}^{M} h_i(z(t)) B_{vi}$$

And, the activation function is selected as follows:

$$h_1 = O_1 O_2, \quad h_2 = O_1 \overline{O}_2, \quad h_3 = \overline{O}_1 O_2, \quad h_4 = \overline{O}_1 \overline{O}_2$$

By considering the pitch angle and the wind speed as scheduling variables, The polytopic Quasi-LPV model (11) is constructed with four vertex linear models derived to represent the system dynamics at four operating points (see Figure 2.(A)):

$$A_i = \begin{bmatrix} b_1 & \frac{B_{dt}}{N_g J_r} & -\frac{K_{dt}}{J_r} & \vartheta_{1i} & 0 & 0 \\ \frac{B_{dt}}{N_g J_g} & \frac{-b_2}{J_g} & \frac{K_{dt}}{N_g J_g} & 0 & \frac{-1}{J_g} & 0 \\ 1 & \frac{-1}{N_g} & 0 & 0 & 0 & 0 \\ 0 & 0 & 0 & 0 & 0 & 1 \\ 0 & 0 & 0 & 0 & \frac{-1}{\tau_g} & 0 \\ 0 & 0 & 0 & -\omega_n^2 & 0 & -2\xi\omega_n \end{bmatrix},$$

$$B = \begin{bmatrix} 0 & 0 \\ 0 & 0 \\ 0 & 0 \\ 0 & 0 \\ 0 & \frac{1}{\tau_g} \\ \omega_n^2 & 0 \end{bmatrix}, \quad B_{vi} = \begin{bmatrix} \vartheta_{2i} \\ 0 \\ 0 \\ 0 \\ 0 \\ 0 \end{bmatrix} \tag{14}$$

where parameters ϑ_i for $i = 1,...,4$ are given in Table 1.

Table 1. Vertex polytope models

Vertex models i	Scheduling function $F_{1i}, F_{2i} \equiv F_i$	Model parameters $\vartheta_{1i}, \vartheta_{2i} \equiv \vartheta_i$	Sub LTI models A_i, B, B_{iv}, C
1	(O_1, O_2)	(D_1, D_2)	A_1, B, B_{1v}, C
2	$(O_1, \overline{O}_2)$	(D_1, d_2)	A_2, B, B_{2v}, C
3	$(\overline{O}_1, O_2)$	(d_1, D_2)	A_3, B, B_{3v}, C
4	$(\overline{O}_1, \overline{O}_2)$	(d_1, d_2)	A_4, B, B_{4v}, C

4. DECENTRALIZED SLIDING MODE OBSERVER MODEL BASED FDI DESIGN

The DSMO design is based on a nonlinear MIMO system subject to actuator faults f_a and sensor faults f_s in the following Quasi-LPV model:

$$\begin{cases} \dot{x} = \sum_{i=1}^{M} h_i(z) \left(A_i x + Bu + B_{vi} v + E_i f_a \right) \\ y = Cx + f_s \end{cases} \tag{15}$$

$$\text{such that : } \begin{cases} \sum_{i=1}^{M} h_i(z) = 1 \\ 0 \le h_i(z) \le 1 \quad \forall i = \{1,...,M\} \end{cases}$$

where $x(t) \in \Re^n$ is the state vector, $u(t) \in \Re^m$ is the input vector, $f_a(t) \in \Re^l$ is an actuator fault, $f_s(t) \in \Re^p$ is a sensor fault and $y(t) \in \Re^p$ is the measurable vector output. For the *ith* local model $A_i \in \Re^{n \times n}$ is the state matrix, $B \in \Re^{n \times m}$ is the matrix of inputs, $E_i \in \Re^{n \times l}$ denotes the full rank fault distribution and $C \in \Re^{p \times n}$ is the matrix of output. Finally, z represents the scheduling vector which is formed by a subset of the input and/or the measurable state variables to define the validity regions of the local models.

The reconstruction of the state variables consists to use the information provided by the input and output signals. The proposed observer for the multiple model (14) is a linear combination of local observers, each of them having the structure proposed by Walcott and Zak [27]. In this context, we consider that the inputs $f_a(t)$ are bounded, such as

$\|f_a(t)\| \le \eta$, where η is scalar and $\|\ .\ \|$ represents the Euclidean norm. It is also assumed that there exists matrices $G_i \in \Re^{n\times p}$, such that $A_{0i} = A_i - G_i C$ have stable eigenvalues and that there exists Lyapunov pairs (P, Q_i) of matrices and other matrices $F_i \in \Re^{p\times n}$ respecting the following structural constraints:

$$\begin{cases} A_{0i}^T P + P A_{0i} = -Q \\ F_i C = R_i^T P, \quad \forall i \in 1,...;M \end{cases} \tag{16}$$

The proposed observer has the following form:

$$\begin{cases} \dot{\hat{x}} = \sum_{i=1}^{M} h_i(z)\left(A_i \hat{x} + Bu + B_{vi} v + E_i f_a + G_i e_y + R_i v_i\right) \\ y = C\hat{x} \end{cases} \tag{17}$$

where e_y is the output error defined as follows:

$$e_y = y - \hat{y} = C(x - \hat{x}) = Ce \tag{18}$$

With $e(t)$ represent the state estimation error, such as:

$$e(t) = x(t) - \hat{x}(t) \tag{19}$$

The matrices G_i and the control variables v_i, with $v_i(t) \in \Re^q$ must be determined in order to guarantee the asymptotic convergence of $\hat{x}(t)$ towards $x(t)$. The terms $v_i(t)$ compensate errors due to the unknown inputs. The dynamic of state estimation error is given as follows:

$$\dot{e} = \sum_{i=1}^{M} h_i(z)\left((A_i - G_i C)e + B_{vi} v + E_i f_a - R_i v_i\right) \tag{20}$$

Theorem 1: The state estimation error between the multiple model (14) and the robust state multiple observer (16) converges to zero, if $v_i(t)$ are given by the following equation:

$$\begin{cases} \text{if } e_y(t) \neq 0, \quad \text{then} \quad v_i(t) = \eta \dfrac{F_i e_y}{\|F_i e_y\|} \\ \text{if } e_y(t) = 0, \quad \text{then} \quad v_i(t) = 0 \end{cases} \tag{21}$$

And if there exist a symmetric definite positive matrix P which satisfies the following inequalities:

$$\begin{aligned} &(A_i - G_i C)^T P + P(A_i - G_i C) < 0 \\ &i = \{1,...,M\} \end{aligned} \tag{22}$$

Proof: To show the asymptotic convergence of this multiple observer, let us consider the following Lyapunov function:

$$V(e(t)) = e^T(t) P e(t) \tag{23}$$

Its derivative in respect to time, evaluated along the trajectory of the system by using equations (17) and (19), may be expressed as:

$$\dot{V} = \sum_{i=1}^{M} h_i(z)\left(e^T(\bar{A}_i^T P + P\bar{A}_i)\right)e + 2e^T P R_i \bar{u} - 2e^T P R_i v_i \tag{24}$$

where: $\bar{A} = A_i - G_i C$

Using the second part of constraint (15), the derivative of the Lyapunov function becomes:

$$\begin{aligned} \dot{V} &= \sum_{i=1}^{M} h_i(z)\left(e^T(\bar{A}_i^T P + P\bar{A}_i)e + 2e^T C^T F_i^T \bar{u} - 2e^T C^T F_i^T v_i\right) \\ &= \sum_{i=1}^{M} h_i(z)\left(e^T(\bar{A}_i^T P + P\bar{A}_i)e + 2e_y{}^T F_i^T \bar{u} - 2e_y{}^T F_i^T v_i\right) \\ &\le \sum_{i=1}^{M} h_i(z)\left(e^T(\bar{A}_i^T P + P\bar{A}_i)e + 2\eta\|F_i\ e_y\| - 2e_y{}^T F_i^T v_i\right) \end{aligned}$$

Using the relation (20), the derivative of the Lyapunov function becomes as follows:

$$\begin{aligned} &\dot{V} \le \sum_{i=1}^{M} h_i(z)\left(e^T(\bar{A}_i^T P + P\bar{A}_i)e + 2\eta\|F_i\ e_y\| - 2\eta e_y{}^T F_i^T \frac{F_i e_y}{\|F_i e_y\|}\right) \\ &\dot{V} \le \sum_{i=1}^{M} h_i(z)\left(e^T(\bar{A}_i^T P + P\bar{A}_i)e\right) \end{aligned} \tag{25}$$

Then, the state estimation error of the robust multiple observer (16) converges to zero if the relation (21) holds.

4.1. Actuator fault reconstruction

The goal of this section is to generate residuals that reflect the faults acting on the system (14). An ideal residual signal should converge to zero in the fault-free case and should diverge from zero when fault occurs. Once a fault has been detected, it must be estimated.

The fault estimation will specify the type of fault, its duration, its amplitude and eventually its probable evolution.

Both the generator and pitch systems can fail, the generator fault can result in an offset and the considered pitch actuator faults are: pump wear, hydraulic leakage, high air content in the hydraulic oil, valve blockage, and pump blockage.

In this case, the examined fault is high air content in the oil. Air is much more compressible than oil; it provokes an overshoot in the transient response because of the higher hydraulic oil elasticity.

The normal air content in the hydraulic oil is 7%, while high air content in the oil corresponds to 15%, therefore the fault is modelled by changing the dynamics of the pitch actuator parameters ω_n and ξ from their nominal values to their faulty values in Eq (6). The parameters for the faulty pitch actuator are shown in Table 2 [15].

Table 2. Parameters for the pitch system under different conditions

Faults	$\omega_n\,(rad/s)$	ξ
Fault-free	11.11	0.6
High air content in oil	5.73	0.45
Pump wear	7.27	0.75
Hydraulic leakage	3.42	0.9

The DSMO is used in this part to detect and reconstruct parameter faults in the pitch and generator dynamics of WTs model

$$\begin{pmatrix}\dot{\beta}\\ \ddot{\beta}\end{pmatrix}=\begin{bmatrix}0 & 1\\ -\omega_n^2 & -2\xi\omega_n\end{bmatrix}\begin{pmatrix}\beta\\ \dot{\beta}\end{pmatrix}+\begin{pmatrix}0\\ \omega_n^2\end{pmatrix}\beta_r \tag{26}$$

$$\dot{T}_g(t)=\frac{1}{\tau_g}\left(T_{g,r}-T_g\right) \tag{27}$$

Alterations in the actuator dynamics of pitch angle and generator torque can be examined by means of changes in the parameters (ω_n and ξ) and time constant τ_g respectively. Actuator offset faults can be modelled by adding an offset to the input signal [14]:

$$a_1 := \omega_n^2, \qquad \longrightarrow \tilde{a}_1 = a_1 + \Delta a_1, \tag{28}$$

$$a_2 := 2\xi\omega_n, \qquad \longrightarrow \tilde{a}_2 = a_2 + \Delta a_2 \tag{29}$$

With: $\tilde{a}_1$ and $\tilde{a}_2$ is a sum of the nominal value (a_1, a_2) and an offset value $(\Delta a_1, \Delta a_2)$.

The altered pitch dynamics is then given by

$$\begin{pmatrix}\dot{\beta}\\ \ddot{\beta}\end{pmatrix}=\begin{bmatrix}0 & 1\\ -a_1 & -a_2\end{bmatrix}\begin{pmatrix}\beta\\ \dot{\beta}\end{pmatrix}+\begin{pmatrix}0\\ a_1\end{pmatrix}\beta_r + \begin{bmatrix}0 & 1\\ -\Delta a_1 & -\Delta a_2\end{bmatrix}\begin{pmatrix}\beta\\ \dot{\beta}\end{pmatrix}+\begin{pmatrix}0\\ \Delta a_1\end{pmatrix}\beta_r \tag{30}$$

Analogously, altered generator torque dynamics can be examined using the reciprocal value a_g of the time constant τ_g.

$$a_g := \frac{1}{\tau_g}, \qquad \longrightarrow \tilde{a}_g = a_g + \Delta a_g \tag{31}$$

$$\dot{T}_g(t) = -a_g T_g + a_g T_{g,r} - \Delta a_g T_g + \Delta a_g T_{g,r} \tag{32}$$

Defining the offset matrices ΔA, and ΔB as:

$$\Delta A=\begin{bmatrix}0_{n-2\times n-2} & 0_{n-2\times 1} & 0_{n-2\times 1}\\ 0_{1\times n-2} & -\Delta a_g & 0\\ 0_{1\times n-3} \quad -\Delta a_1 & 0 & -\Delta a_2\end{bmatrix}, \quad \Delta B=\begin{bmatrix}0_{n-2\times 1} & 0_{n-2\times 1}\\ 0 & \Delta a_g\\ \Delta a_1 & 0\end{bmatrix}$$

where n denotes the observer states system number, the observer system dynamics (without feedback terms) with modified actuator dynamics can be written as [16]:

$$\dot{x}(t)=\sum_{i=1}^{M} h_i(z)\left(A_i x + Bu + B_{vi} v + \Delta A x + \Delta B u\right) \tag{33}$$

In order to reconstruct the altered dynamics parameters Δa_1 , Δa_2 and Δa_g , a fault matrix E and an actuator fault vector f_a must be found such that:

$$\begin{aligned} Ef_a &= \Delta A x + \Delta B u \\ &= \left(0 \quad \ldots \quad 0 \quad \Delta a_g (T_{g,r} - T_g) \quad \Delta a_1(\beta_r - \beta) \quad -\Delta a_2 \dot{\beta}\right)^T \end{aligned}$$

Choosing:

$$E=\begin{bmatrix}0 & \ldots & 1 & 0\\ 0 & \ldots & 0 & 1\end{bmatrix}^T \text{ and } \quad f_a=\begin{pmatrix}\Delta a_g(T_{g,r}-T_g)\\ \Delta a_1(\beta_r-\beta)-\Delta a_2\dot{\beta}\end{pmatrix}$$

Both the torque actuator fault Δa_g and the pitch actuator faults Δa_1 and Δa_2 can be reconstructed. The reconstructed actuator fault vector is thus given by:

$$\hat{f}_a=\begin{pmatrix}\Delta\hat{a}_g(T_{g,r}-T_g)\\ \Delta\hat{a}_1(\beta_r-\beta)-\Delta\hat{a}_2\dot{\beta}\end{pmatrix}$$

5. SIMULATION RESULTS

The simulation tests use the WT benchmark system proposed by kk-electronic [13].

It is a three blade horizontal axis variable speed WT with full converter coupling.

The operated ranges of pitch angle is $0.01 \le \beta \le 0.03$ (rad) and the range of wind speed is $11 \le v \le 17$ (m/s).

The membership functions of the scheduling variables are depicted in figure 3.

The local dynamic models are deduced from the nonlinear model (1) through dynamic linearization about operating points. Figure 4 shows the WECS state variables in real and estimation case

In order to identify the actuator faults in the pitch angle and generator torque, a DSMO described in section 4, is used to estimate these faults.

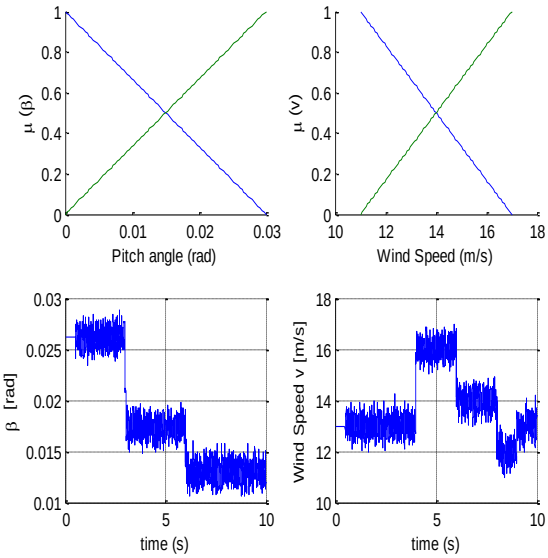

Figure 3. Scheduling variables: triangular membership functions (top) and temporal evolutions (bottom)

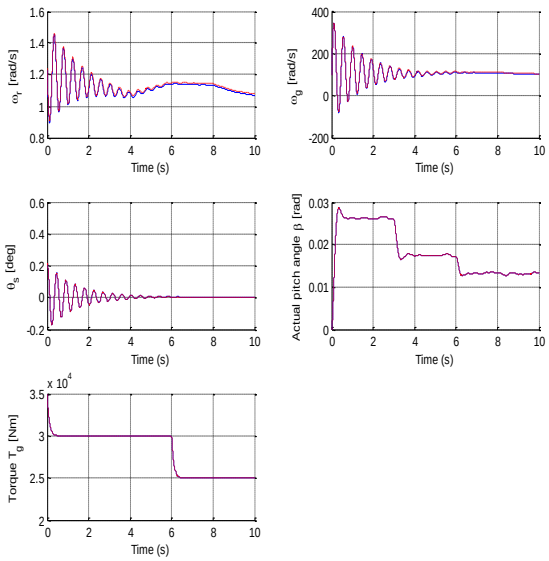

Figure 4. Evolution of real (solid blue line) and estimated states (dotted red line) of WECS based DSMO

The reconstruction of actuator faults is based on the analysis of the residuals generated by the DSMO. High air content in the oil that represented a fault actuator in pitch angle has been added between 6s and 7s.

For the generator torque an offset of 10000 [Nm] was active between 5.5s and 6.5s.

The top of Figure 5 and Figure 6 illustrates the actual pitch angle and generator torque with and without faults scenario.

The components of the reconstructed fault vector $\hat{f}_a$ based on DSMO are depicted in the bottom of Figure 5 and Figure 6. It can be seen that both actuators faults are reasonably well reconstructed. Short peaks occur when the fault are switched on/off.

The fault detection and reconstruction times for pitch angle and generator torque are approximately 0.48s and 0.36s, respectively. The DSMO is, therefore, a very short and efficient method for detecting and reconstructing the actuator faults.

For a pitch angle sensor fault an additive gain factor (1.5 rad) had been added between 4 s and 5 s.

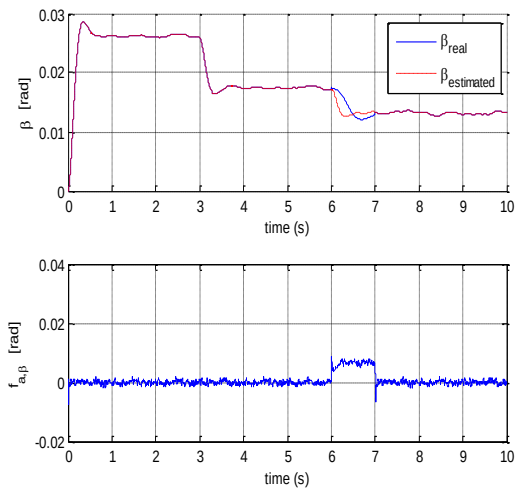

Figure 5. Actual pitch angle with and without fault (top) and the reconstructed actuator fault vector (β) (bottom)

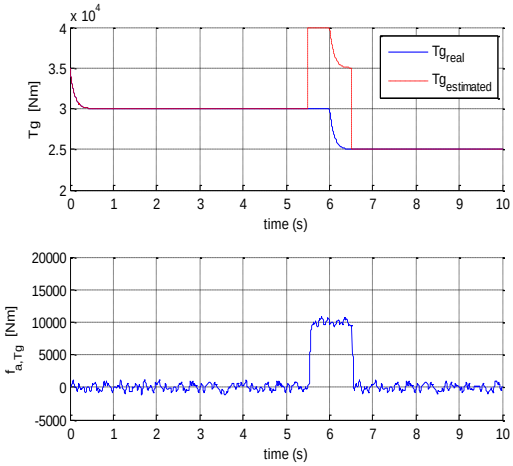

Figure 6. Actual generator torque with and without fault (top) and the reconstructed actuator fault vector (T_g) (bottom)

The actual pitch angle with and without the sensor fault is given by the top of Figure 7. The bottom of Figure 7 demonstrates that the residual is not zero without fault due to the presence of sensor noise; the residual is significantly increases after the fault occurs. The fault is detected, isolated, and reconstructed in approximately 0.26 s.

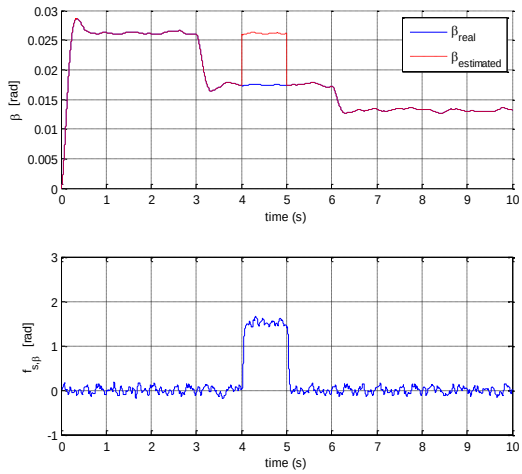

Figure 7. Actual pitch angle with and without fault (top) and the reconstructed sensor fault vector (β) (bottom)

6. CONCLUSIONS

In this paper, a condition monitoring system based on decentralized sliding mode observer (DSMO) is used to automate the diagnosis process of variable speed wind energy turbine. In this robust observer, stability is guaranteed by a quadratic lyapunov function. A polytopic Quasi-LPV model describing the dynamics of the WT is derived. It depends on two scheduling variables: the pitch angle and the wind speed. The nonlinear system behaviour is approximated using four vertex linear systems derived to represent the system dynamics at four operating points by using the polytopic convex transformation.

The DSMO is used to detect and reconstruct sensor and

actuator parameter faults in the WT. It permits the detection and localisation by means of reconstruction of pitch angle sensor fault and any fault that implies a change in the dynamics of the pitch actuator system almost instantly. The performance of this observer was evaluated and we can confirm its efficiency. Finally, further work could be the practical implementation possibilities of this strategy.

ACKNOWLEDGMENT

The authors would like to gratefully acknowledge the Laboratory of Automatic and Signals Annaba (LASA), Badji Mokhtar University, P.O. Box 12, Annaba 23000, Algeria.

REFERENCES

[1] Piyali G, Akhtar K, Aladin Z.(2017). Optimum fuzzy logic control system design using cuckoo search algorithm for pitch control of a wind turbine. Advances C 72(4): 266-280.

[2] Arama FZ, Bousserhane IK, Laribi S, Sahli Y, Mazari B. (2018). Artificial intelligence control applied in wind energy conversion system. International Journal of Power Electronics and Drive System (IJPEDS) 9(2): 571-578. https://doi.org/10.11591/ijpeds.v9n2.pp571-578

[3] Fadil H, Elhafyani ML, Zouggar S. (2018). Enhanced three-phase inverter fault detection and diagnosis approach-design and experimental evaluation. International Journal of Power Electronics and Drive System (IJPEDS) 9(2): 559-570. https://doi.org/10.11591/ijpeds.v9n2.pp559-570

[4] Chen F, Fu ZG. (2016). Wind turbine failure risk assessment model based on DBN. Advances C 71(1): 110-124.

[5] Boumaiza A, Arbaoui F, Saidi ML. (2014). Diagnostic des défauts à base d'observateur dans un système éolien. Mediterranean Journal of Modeling and Simulation 1(1): 045-055.

[6] Park JH, Park GT. (2003). Adaptive fuzzy observer with minimal dynamic order for uncertain nonlinear systems. IEEE Proceedings Control Theory and Applications 150(2): 189-197. https://doi.org/10.1049/ip-cta:20030148

[7] Shaker MS, Patton RJ. (2014). Active sensor fault tolerant output feedback tracking control for wind turbine systems via TS model. Engineering Applications of Artificial Intelligence 34: 1-12.

[8] Boussairi Y, Abouloifa A, Lachkar I, Hamdoun A, Aouadi C. (2018). Modeling and nonlinear control of a wind turbine system based on a permanent magnet synchronous generator connected to the three-phase network. International Journal of Power Electronics and Drive System (IJPEDS) 9(2): 766-774. http://doi.org/10.11591/ijpeds.v9.i2.pp%25p

[9] Edwards C, Spurgeon SK. (2000). Sliding mode observers for fault detection and isolation. Automatica. 36(4): 541-553. https://doi.org/10.3182/20020721-6-ES-1901.00789

[10] Tan CP, Edwards C. (2001). An LMI approach for designing sliding mode observers. Int. J. Control. 74: 1559-1568. https://doi.org/10.1080/00207170110081723

[11] Walcott BL, Zak SH. (1987). State observation of nonlinear uncertain dynamical systems. IEEE Trans. Automat. Control 32: 166-170. https://doi.org/10.1109/TAC.1987.1104530

[12] Ben Hamouda L, Bennouna OAM, Langlois N. (2013). Quasi-LPV model predictive reconfigurable control for constrained nonlinear systems. Conference on Control and Fault-Tolerant Systems (SysTol), Nice, France.

[13] Odgaard F, Johnson K. (2013). Wind turbine fault detection and fault tolerant control – an enhanced benchmark challenge. American Control Conference (ACC), 4447-4452.

[14] Dari H, Mehenaoui L, Ramdani M. (2015). An optimized fuzzy controller to capture optimal power from wind turbine. 4th International Conference on Renewable Energy Research and Applications, Italy, pp. 815-820.

[15] Esbensen T, Sloth C. (2009). Fault diagnosis and fault-tolerant control of wind turbines. Master's Thesis, Department of Electronic Systems, Aalborg University, Denmark.

[16] Georg S, Schulte H. (2014). Diagnosis of actuator parameter faults in wind turbines using a takagi-sugeno sliding mode observer. Intelligent Systems in Technical and Medical Diagnostics. Springer, Berlin, Heidelberg, 230. https://doi.org/10.1007/978-3-642-39881-0_2

NOMENCLATURE

β_{dt}	The torsion damping coefficient $\left[Nm/(rad/s)\right]$
B_g	Viscous friction of high-speed shaft $\left[Nm/(rad/s)\right]$
B_r	Viscous friction of low-speed shaft $\left[Nm/(rad/s)\right]$
J_g	Inertia of the high-speed shaft $\left[kgm^2\right]$
J_r	Inertia of the low-speed shaft $\left[kgm^2\right]$
K_{dt}	The torsion stiffness $\left[Nm/rad\right]$
N_g	The drive train gear ratio $\left[Nm/(rad/s)\right]$
$T_a(t)$	The aerodynamic torque $\left[Nm\right]$
$T_g(t)$	The generator torque $\left[Nm\right]$
ω_r	The rotor speed $\left[rad/s\right]$
ω_g	The generator speed $\left[rad/s\right]$
$\theta_\Delta(t)$	Torsion angle of the drive train $\left[rad\right]$

Subscripts

DSMO	Decentralized sliding mode observer
Quasi-LPV	Quasi linear parameter varying
SMO	Sliding mode observer
VSWECS	Variable speed wind energy conversion system
WECS	Wind energy conversion systems
WT	Wind turbines